Egyptian Journal of Petroleum (2015) **24**, 1–11

HOSTED BY

Egyptian Petroleum Research Institute

Egyptian Journal of Petroleum

www.elsevier.com/locate/egyjp
www.sciencedirect.com

FULL LENGTH ARTICLE

Study on P-wave and S-wave velocity in dry and wet sandstones of Tushka region, Egypt

Mohamed A. Kassab [a,*], **Andreas Weller** [b]

[a] *Egyptian Petroleum Research Institute, 11727, El Zohour Region, Naser City, Cairo, Egypt*
[b] *Institute of Geophysics, Clausthal University of Technology, D-38678 Clausthal-Zellerfeld, Germany*

Received 21 November 2013; accepted 30 January 2014
Available online 11 April 2015

KEYWORDS

P-wave velocity;
S-wave velocity;
Porosity;
Permeability;
Density;
Sandstone

Abstract Acoustic laboratory measurements have been conducted for forty-two sandstone samples at fully air and water saturation. This study is an attempt to learn more about the behavior of both P-wave and S-wave velocity in porous sandstone rock samples for both dry and wet conditions.

The statistical analysis indicates that higher values of the P-wave velocity are obtained for saturated samples and lower values are obtained for dry samples. The average P-wave velocity of dry rock samples is 2766 m/s and the average P-wave velocity of wet rock samples is 2950 m/s. The S-wave velocity is higher in the dry state with an average value of 1585 m/s. The average S-wave velocity of wet rock samples is 1357 m/s.

The derived equations can be used for the prediction of P-wave velocity of wet rock samples from the P-wave velocity of dry rock samples, and the S-wave velocity of wet rock samples can be predicted from the S-wave velocity of dry rock samples. A strong linear correlation between P-wave velocity and S-wave velocity of dry rock samples and between P-wave velocity and S-wave velocity of wet rock samples was found. The resulting linear equations can be used for the estimation of S-wave velocity from the P-wave velocity in the case of both dry and wet rock samples.

1. Introduction

Forty-two Nubian sandstone samples originate from Tushka region in the South Western Desert. The samples were collected from outcropping formations of Cretaceous age. According to Thabit [25] the studied Nubian sandstones can be distinguished from base to top into four formations as follows: Adindan Formation (Jurassic–Valanginian), Abu Simbil Formation (Valanginian–Barremian), Abu Ballas Formation (Aptian–Albian) and Kesieba Formation (Campanian–Maastrichtian). Kesieba Formation is separated from the underlying Abu Ballas Formation by a disconformity of regional extent caused by the removal of the Sabayia Formation during a tectonic exhumation. The study area is located between latitudes N 22° 15′ and N 22° 35′ and longitudes E 31° 00′ and E 31° 40′. The Nubian sandstones are of special interest due to their economic oil and gas potentiality, groundwater

* Corresponding author.
E-mail addresses: mkassab68@yahoo.com, mohamedkassab1968@hotmail.com (M.A. Kassab), andreas.weller@tu-clausthal.de (A. Weller).

Peer review under responsibility of Egyptian Petroleum Research Institute.

http://dx.doi.org/10.1016/j.ejpe.2015.02.001

resources and mineral deposits such as kaolinite, coal, glass sand, uranium, copper, iron, and manganese ores [2,6 and 7].

The ultrasonic wave velocity in rock sample is related to its elastic coefficients, internal structure and density. Hicks and Berry [14] list the parameters influencing velocities in rocks which may be summarized as follows; (1) Rock framework as elastic constant of grains, density of grains, type of cementing material, pressure on skeleton lithology and porosity, (2) Fluid contained in pore spaces as density of fluid, pressure on fluid, and compressibility of fluid and (3) Temperature of medium, where the change in temperature over the range from 25–150 °C causes velocity change in dry rock either shale or sandstone causing 5–7% reduction in velocity for saturated cores under equal hydrostatic and skeleton pressure [15]. (4) Depth and elevated overburden pressure, where the velocity increases logarithmically with increasing in depth and rock pressure as well [5]. The overburden pressure increases seismic velocity, while its associated high temperature decreases it.

Han et al. [13] studied the effect of clay content on wave velocities and concluded that clay content is the next most important parameter to porosity in reducing velocities. Minear [19] showed that clay suspended in the pores of sandstone has only a small effect on velocities, whereas both structure and laminated clay result in a dramatic velocity reduction.

Clay content is the next most important parameter in reducing velocities, whereas both structure and laminated clay result in a dramatic velocity reduction. The presence of pore space reduces the bulk density of the rock. This would appear to increase P-wave and S-wave velocity due to the reduction in density. The effect of a general decrease in P-wave and S-wave velocity with increasing porosity is due to the increase in porosity reducing the rigidity of the rock that decreases both P-wave and S-wave. Pore structure has an effect on both bulk and shear modulus [12].

The shear wave velocity values in a liquid–wet porous material will always be less than that in the dry material based on an assumption that micro-cracks are negligible. The compressional wave velocity in the liquid–wet porous material will generally be higher than that in the dry case, except for material having low bulk compressibility [3]. High values of the P-wave velocity are obtained for saturated samples and low values are obtained for dry samples (P-wave velocity (dry) < P-wave velocity (saturated)) [4]. The shear wave velocity decreases as the water saturation increasing until it reaches 70–75% and then starts to increase again [9]. Poisson's ratio, which has been calculated from acoustics laboratory measurements when the samples are gas, gas–water, and crude oil–water saturated, can be used for step wise tracing of the oil–water transitional zone and detecting its exact thickness in high porosity oil bearing sandstone and/or carbonate reservoir [8]. P-wave velocity of wet rock can be predicted from the P-wave velocity of dry rock [16].

The present work aims to learn more about the behavior of both P-wave and S-wave velocity in sandstone samples for both dry and wet conditions and to investigate the effect of porosity, permeability, both dry and wet densities and saturation on the acoustic velocities.

2. Methods of investigation

Thin sections and scanning electron microscopy (SEM) of core samples are used to identify the mineralogical composition and diagenetic processes. The petrographical study of forty-two thin sections is based mainly on the microscopic examination of the studied samples. Thin section preparation involved vacuum impregnation with blue epoxy to facilitate the recognition of porosity types. SEM analysis was performed by the scanning electron microscopy at the Institute of Geology and Paleontology at Clausthal University of Technology, Germany. The clastic rocks in the present study were classified according to Pettijohn et al. [21] and Folk [10].

All samples were analyzed at the Institute of Geophysics at Clausthal University of Technology, Germany and the Egyptian Petroleum Research Institute, Egypt. Compressional wave velocity (P-wave velocity) and shear wave velocity (S-wave velocity) were measured at room temperature and ambient pressure on cylindrical samples with a diameter of about 2.5 cm and a length of up to 3.5 cm cut from the blocks, by using an equipment of Inspection Technologies (USLT 2000) at ultrasonic frequencies of 500 kHz. The velocity of an ultrasonic wave in rock samples is related to its elastic coefficients, internal structure and density. P-wave velocity (Vp) and S-wave velocity (Vs) measurements were made with the samples in both dry and fully water saturated state, both of them can be computed from the elastic moduli by the following formulas;

$$\mathrm{Vp} = [(\kappa + 4\mu/3)/d]^{1/2} \quad \text{and} \tag{1}$$

$$\mathrm{Vs} = [\mu/d]^{1/2} \tag{2}$$

with κ being the bulk modulus, μ the shear modulus, and d the density.

Porosity (Φ) was measured by use of helium porosimeter. The porosity of a rock is defined as the ratio of the rock void spaces to its bulk volume, multiplied by one hundred to express it in percent [1]. This can be expressed in mathematical form as;

$$\Phi = V_\mathrm{b} - V_\mathrm{g}/V_\mathrm{b} \tag{3}$$

with Φ being the porosity fraction, V_b the bulk volume, cm^3, and V_g the grain volume, cm^3.

The permeability (K) in mD was measured by use of core lab permeameter. Darcy's equation relating permeability to compressible fluids is;

$$K = [2000\mu qL\mathrm{Pa}]/[A(P_1{}^2 - P_2^2)] \tag{4}$$

with K being the permeability (mD), μ the viscosity of air, centipoises, q the gas volume flow rate cm^3/sec, P_1 the upstream pressure (atmosphere), P_2 the downstream pressure (atmosphere) and Pa the atmospheric pressure (atmosphere).

The dry bulk density is defined as the mass per unit volume of a rock in its natural state.

$$d_\mathrm{b} = m_\mathrm{d}/V \tag{5}$$

with d_b being the bulk density in $\mathrm{g/cm}^3$, m_d the dry mass of the sample in g and V the volume of the sample in cm^3.

The grain density was determined as a byproduct of porosity measurements, by using the following equation:

$$d_\mathrm{g} = m_\mathrm{d}/V_\mathrm{g} \tag{6}$$

with d_g being the grain density in $\mathrm{g/cm}^3$ and V_g the volume of grains in cm^3.

The density can be related to porosity by the following equation, according to Schlumberger [24].

Table 1 Porosity, permeability, grain density, dry bulk density, wet bulk density, P-wave velocity and S-wave velocity of dry and wet rock samples.

Sample no.	Φ in fraction	K in mD	d_g in g/cm^3	d_b in g/cm^3	d_w in g/cm^3	Vp-dry in m/s	Vp-wet in m/s	Vs-dry in m/s	Vs-wet in m/s
1	0.311	2285.70	2.65	1.83	2.14	2718.5	2775		
2	0.276	388.83	2.74	1.98	2.26	2819.5	3157		
3	0.253	217.28	2.77	2.07	2.32	3390.5	3427		
4	0.261	263.77	2.79	2.06	2.32	3312	3572	2400.5	2256
5	0.340	4406.44	2.63	1.74	2.08	2402.5	2593		
6	0.335	4728.11	2.63	1.75	2.09	2391.5	2611	1337	1232
7	0.330	5334.62	2.63	1.76	2.09	2288.5			
8	0.285	4265.79	2.62	1.88	2.16	2404	2881		
9	0.272	1432.72	2.64	1.92	2.19	2649	3086		
10	0.276	2890.77	2.64	1.91	2.19	2581.5	2889	1171	1175.5
11	0.346	2736.92	2.65	1.73	2.08	2445	2606	1337	
12	0.330	2476.64	2.65	1.77	2.10	2422.5			
13	0.266	589.61	2.64	1.94	2.20	2639.5			
14	0.314	432.44	2.75	1.89	2.20	2645	2859	1377	1170
15	0.320	615.25	2.74	1.87	2.18	2962.5	3035	1517.5	1293.5
16	0.322	673.99	2.75	1.86	2.19	2619.5	2889	1245	1084.5
17	0.299	33.90	2.67	1.87	2.17	2952.5	2912	1559.5	1310
18	0.262	16.01	2.67	1.97	2.23	2992	2881	1592	1296
19	0.289	139.85	2.67	1.90	2.19	2979	3060		
20	0.343	31.07	2.64	1.73	2.08	2607.5	2668	1746	1117
21	0.322	1090.18	2.65	1.80	2.12	2743.5	2794		
22	0.326	2019.40	2.64	1.78	2.11	2998	2873	2324.5	1820.5
23	0.304	4410.44	2.64	1.84	2.14	2480	2840		
24	0.302	3736.31	2.64	1.84	2.15	2600.5	2646		
25	0.303	4484.17	2.64	1.84	2.14	2712	2772	1708	1521
26	0.251	2153.97	2.65	1.98	2.23	2952			
27	0.261	5012.59	2.65	1.96	2.22	2887.5			
28	0.247	3628.37	2.65	1.99	2.24	3286	3142	1596.5	1393.5
29	0.283	7570.73	2.63	1.89	2.17	2786.5	3061	1353	1212.5
30	0.269	6830.21	2.63	1.92	2.19	2525.5	2993	1311	1217
31	0.284	6689.88	2.64	1.89	2.17	2326	2855	1033.5	1051
32	0.292	1632.53	2.65	1.88	2.17	3192	3201	1709	1473.5
33	0.287	1258.81	2.65	1.89	2.18	3118.5	3095	1513	1374
34	0.269	1135.63	2.65	1.94	2.21	3277	3273		
35	0.292	323.99	2.64	1.87	2.16	2405	2528		
36	0.311	1160.99	2.65	1.83	2.14	2298.5			
37	0.272	0.90	2.80	2.03	2.31	2923	3164	1542.5	1378.5
38	0.347	203.62	2.70	1.77	2.11	2850	2866	2081	1345
39	0.273	7750.01	2.63	1.91	2.18	2950			
40	0.257	4969.19	2.63	1.96	2.21	3365.5	3334	1835	1418
41	0.272	530.89	2.69	1.95	2.23	2525.5			
42	0.201	14.70	2.65	2.12	2.32	2756	2984		

$$d_b = (1 - \Phi)d_m + \Phi d_f \quad (7)$$

with d_m being the density of matrix and d_f the pore fluid density.

Dry bulk density in g/cm^3 was calculated according to Eq. (5) and can be calculated according to the following equation;

$$d_b = (1 - \Phi)d_m + \Phi d_a \quad (8)$$

with d_b being the dry bulk density and d_a the density of air.

Wet bulk density d_w in g/cm^3 is calculated according to the following equation;

$$d_w = (1 - \Phi)d_m + \Phi d_f \quad (9)$$

with d_w being the wet bulk density and d_f the pore fluid (water) density.

Porosity, permeability, grain density, dry bulk density, wet bulk density, P-wave velocity and S-wave velocity of dry and wet rock samples are listed in Table 1 while minimum, maximum, average and standard deviation of porosity, permeability, grain density, dry bulk density, wet bulk density, P-wave velocity and S-wave velocity of dry and wet rock samples are listed in Table 2. Some previously published compressional wave velocity and porosity data for the same Nubian sandstone samples collected from South Western Desert (Tushka region), have been used in a study for estimation of porosity from compressional wave velocity [17]. A similar study has been performed at carbonate samples originating from the Tushka area [18].

3. Results and discussion

3.1. Mineralogical investigations of the studied sandstones

The studied sandstones are composed of quartz grains cemented together by silica, iron oxides and/or clay content. Because

Table 2 Minimum, maximum, average and standard deviation of porosity, permeability, grain density, dry bulk density, wet bulk density, P-wave velocity and S-wave velocity of dry and wet rock samples.

	Φ in fraction	K in mD	d_g in g/cm^3	d_b in g/cm^3	d_w in g/cm^3	Vp-dry in m/s	Vp-wet in m/s	Vs-dry in m/s	Vs-wet in m/s
Minimum	0.201	0.90	2.624	1.731	2.076	2289	2528	1034	1051
Maximum	0.347	7750.01	2.795	2.118	2.321	3391	3572	2401	2256
Average	0.292	2394.46	2.666	1.888	2.179	2766	2950	1585	1357
Standard deviation	3.18	2294.14	0.046	0.093	0.064	308	242	343	267

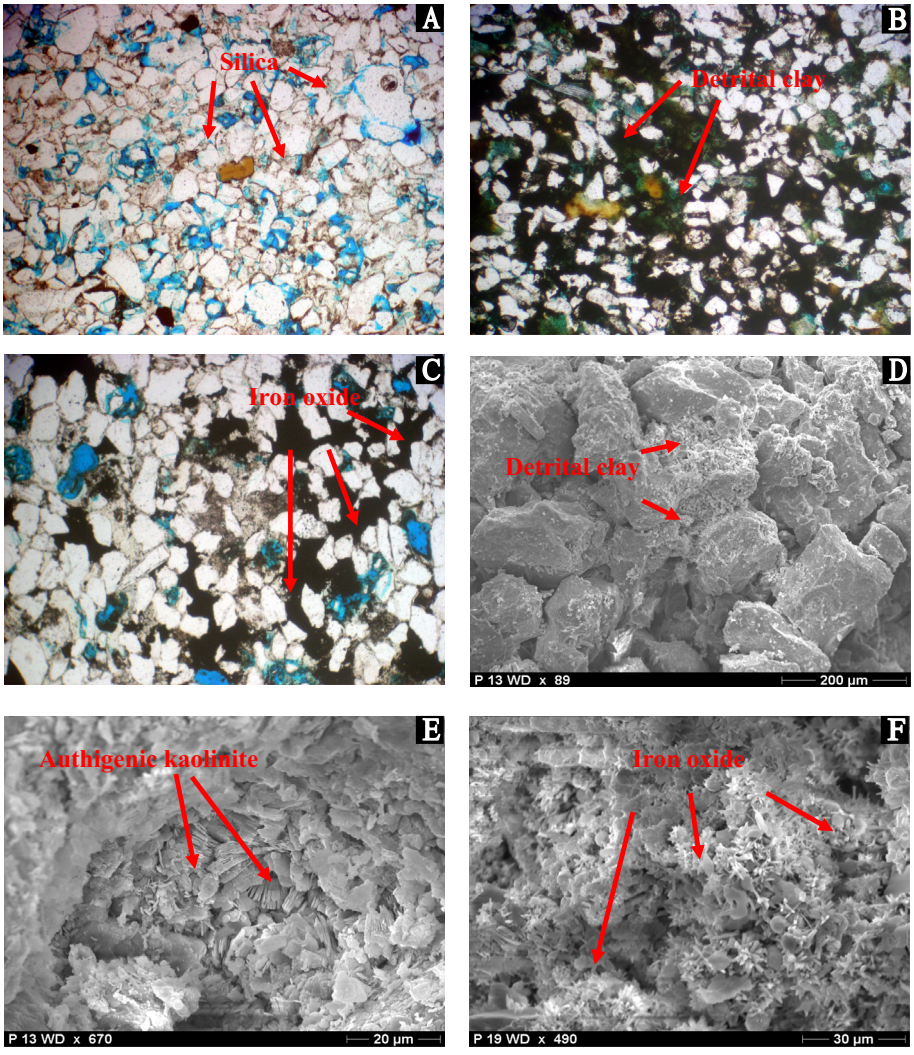

Plate 1 Photomicrographs of Nubian sandstones from type sections in south Egypt, the injected resin filling pores is dyed blue; (A) Quartz arenite, intensive dissolution of quartz grains increasing the fracture and intragranular porosity, X-40, PPL, (B) Quartz wacke, detrital clay partially filling pore spaces and cementing the quartz grains, X-40, PPL, (C) Ferruginous quartz arenite, iron oxide patches masking micro/matrix and intergranular porosity, X-40, PPL, (D) Some detrital clay partially filling pore spaces and cementing the quartz grains, (E) Some authigenic kaolinite booklets partially filling the pore spaces and (F) Some iron oxide filaments rose-like structure.

of the varying clay contents this sandstone can be regarded as shaly sandstone. Detailed petrographical analysis of the sandstone samples originating from Tushka region in the South Western Desert was performed by Nabawy et al. [20]. Petrographically, these sandstones are composed of ill sorted, fine to coarse and rounded to angular quartz grains cemented together by silica cement, iron oxides and/or clay content. These sandstones are mainly quartz arenite (Plate 1A), quartz wacke (Plate 1B) and ferruginous quartz arenite (Plate 1C). Some iron oxides, mostly as pigments, much iron oxide patches masking micro/matrix and intergranular porosity and clay content are disseminated within the cement, partially filling and lining the pore spaces and sometimes cementing the quartz grains together. The quartz grains are mostly in point

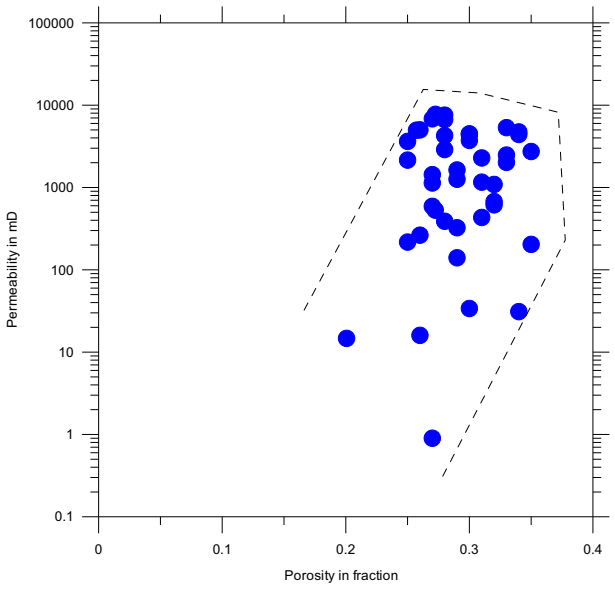

Figure 1 Relationship between porosity and permeability.

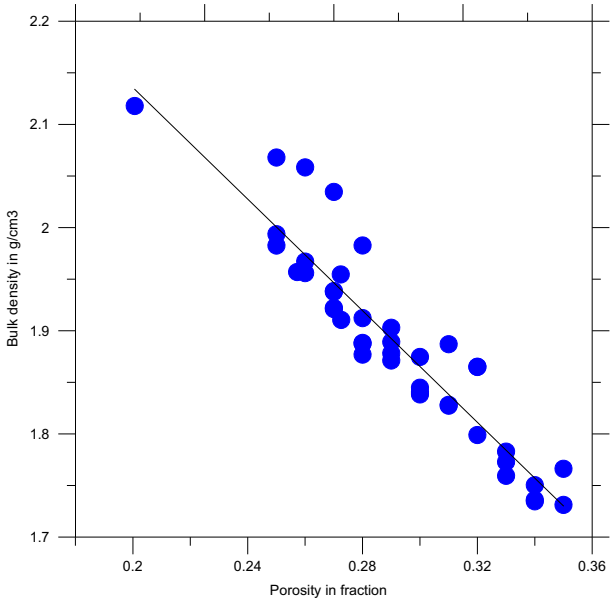

Figure 2 Relationship between porosity and dry bulk density.

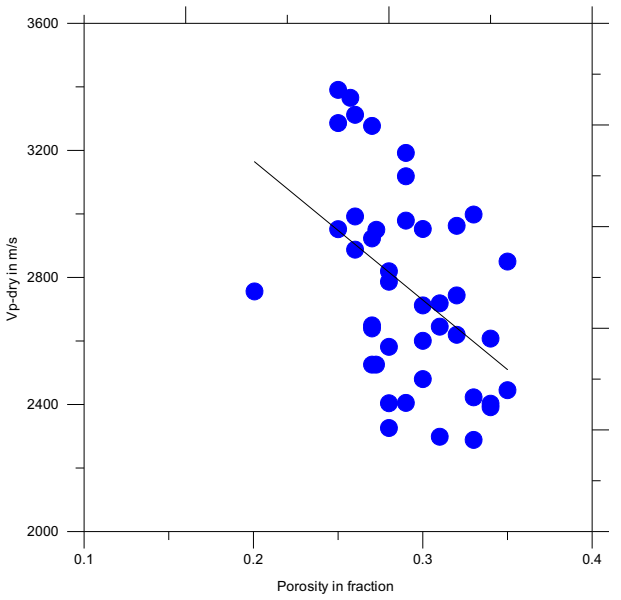

Figure 3 Relationship between porosity and P-wave velocity of dry rock samples.

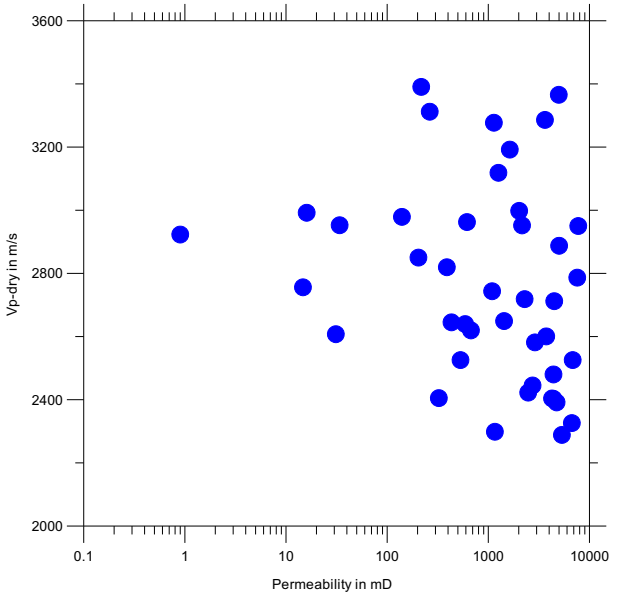

Figure 4 Relationship between permeability and P-wave velocity of dry rock samples.

contact, and sometimes in suture or concave–convex contact. Some detrital clay (Plate 1D and B), partially filling pore spaces and cementing the quartz grains. Some authigenic kaolinite booklets partially filling the pore spaces (Plate 1E) and some iron oxide filaments rose-like structure (Plate 1F).

Diagenetic signatures observed in the studied sandstones include compaction, cementation and dissolution.

There are several features indicating that the investigated sandstones have been subjected to considerable compaction, fractured quartz grains, sometimes internally deformed, and the suture or concave–convex contact between quartz grains (Plate 1A).

Major diagenetic minerals and cements recognized in these sandstones are silica, iron oxides, and/or clay content. Cementations with iron oxides and silica are the common diagenetic feature in most of the investigated sandstones. Detrital clay partially filling pore spaces and cementing the quartz grains and some authigenic kaolinite booklets partially filling the pore spaces are present in some of the studied sandstone samples.

Cementation by silica (Plate 1A) attached the grains together, sometimes slightly reducing porosity values. Some iron oxides, mostly as pigments (Plate 1C) and clay content are disseminated within the cement, partially filling and lining the pore spaces and sometimes cementing the quartz grains together (Plate 1B, D and E).

On the other side, dissolution and leaching out of quartz, clay contents and feldspar are the main porosity-enhancing

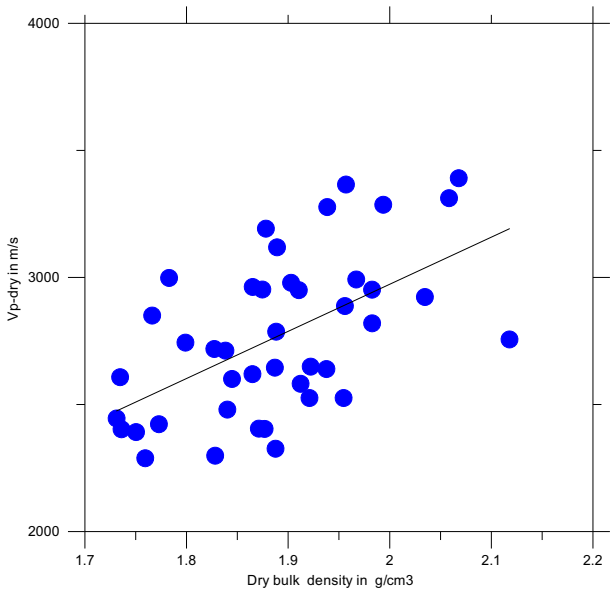

Figure 5 Relationship between P-wave velocity and dry bulk density of dry rock samples.

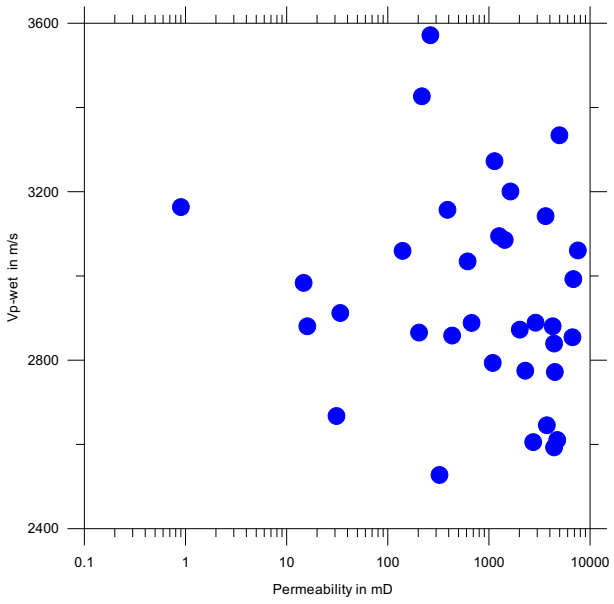

Figure 7 Relationship between permeability and P-wave velocity of wet rock samples.

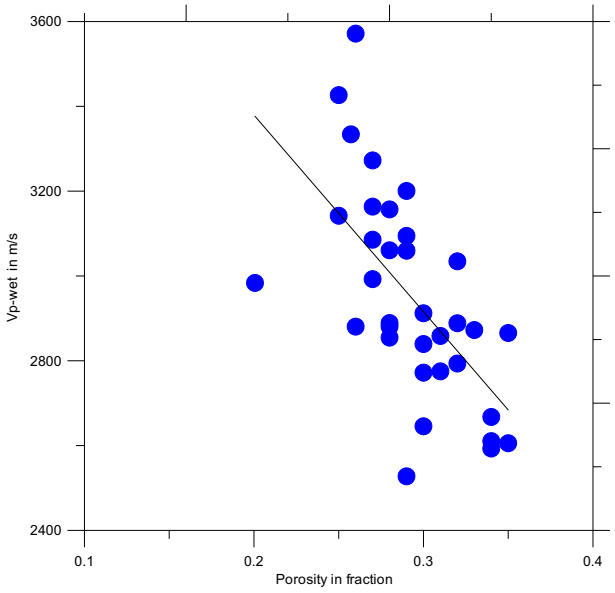

Figure 6 Relationship between porosity and P-wave velocity of wet rock samples.

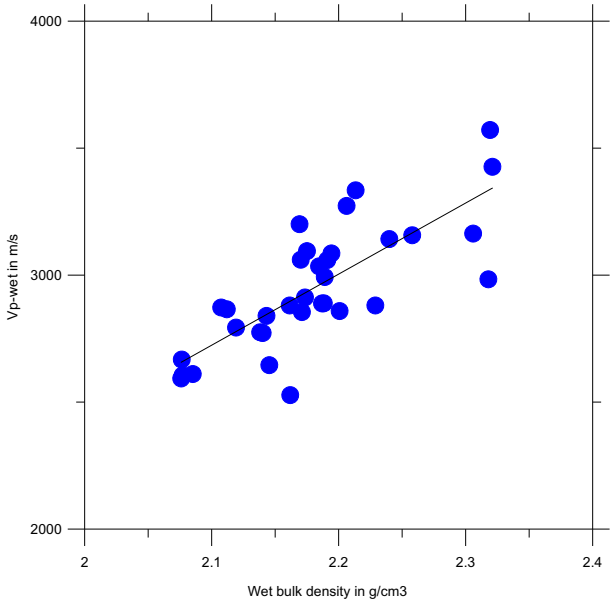

Figure 8 Relationship between P-wave velocity and wet bulk density of wet rock samples.

diagenetic factors giving rise to excellent porosity (Plate 1A) and permeable paths for pore fluid movement.

The pore spaces of the Nubian sandstone samples could be separated into: (1) intergranular porosity (Plate 1A and D), fracture and intragranular porosity (Plate 1A and C) and matrix porosity, masked by the iron oxides (Plate 1B and C).

3.2. Density, porosity and permeability

The obtained grain density varies from 2.62 to 2.80 g/cm^3 with mean values 2.67 g/cm^3 and standard deviation 0.046 g/cm^3. The obtained dry bulk density values vary from 1.73 to 2.12 g/cm^3 with mean values 1.89 g/cm^3 and standard deviation 0.093 g/cm^3. The wet bulk density values vary from 2.08 to 2.32 g/cm^3 with mean values 2.18 g/cm^3 and standard deviation 0.064 g/cm^3. The measured porosity values vary from 0.201 to 0.347 with mean values 0.292 and standard deviation 3.18%, while the permeability value distribution varies from 0.900 mD to 7750 mD, with mean values 2394 mD and standard deviation 2294 mD. Sandstone samples of the Tushka region were integrated in a study comparing different models of permeability prediction using the transverse relaxation time of nuclear magnetic resonance data and parameters determined from spectral induced polarization [26].

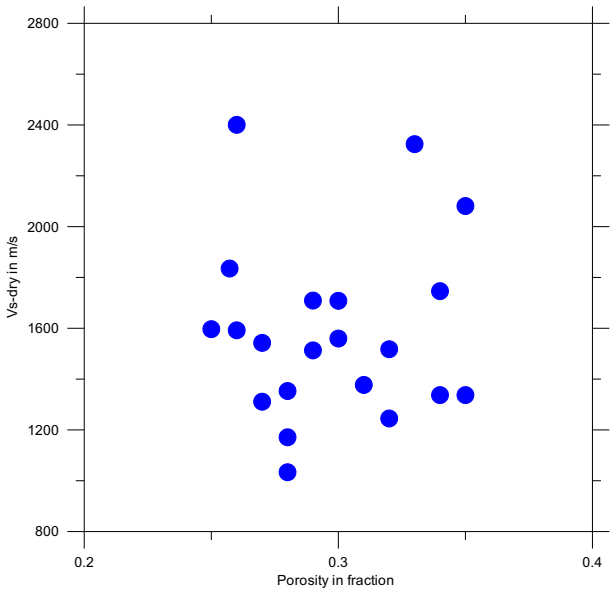

Figure 9 Relationship between porosity and S-wave velocity of dry rock samples.

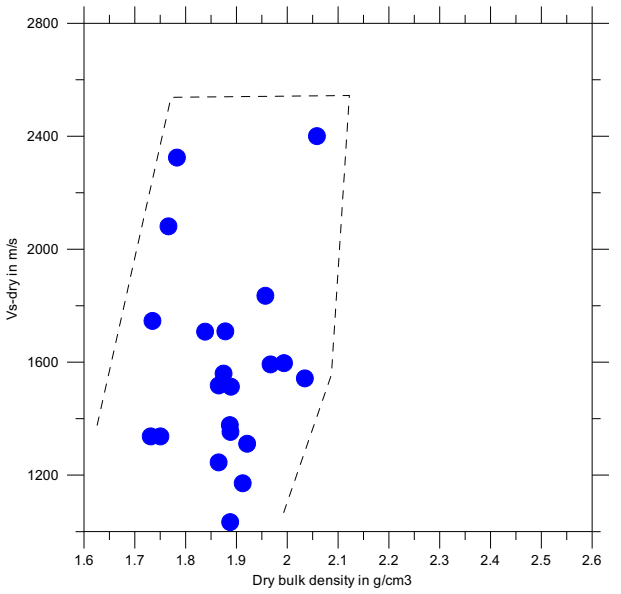

Figure 11 Relationship between S-wave velocity and dry bulk density of dry rock samples.

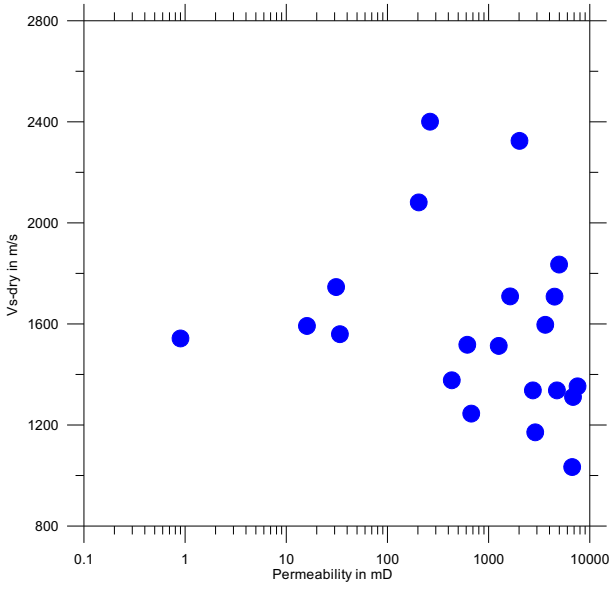

Figure 10 Relationship between permeability and S-wave velocity of dry rock samples.

3.2.1. Density–porosity relationship

The dry bulk density and porosity relationship for dry samples was studied as an attempt to perform a reliable relationship to be utilized for porosity prediction in sandstone reservoirs. This relationship, which is shown in Fig. 2, indicates a decrease of porosity with increasing the dry bulk density as predicted by Eq. (8) with vanishing density of the air. This relationship is characterized by a very good coefficient of correlation (r = 0.93) and indicates that porosity can be predicted from bulk density, with a high precision.

3.2.2. Porosity–permeability relationship

The relationship between permeability and porosity Fig. 1 for the studied rock samples is indicated by a positive trend, which means that the porosity is not the main contributor for the rock permeability. The fine contents and/or differences in pore throat sizes seem to be the main controls of permeability. The relationship between porosity and permeability for the rock samples is affected by cementation with silica, iron oxides and clay content, (Plate 1A, B, D and E). Based on the obtained results, the pore filling silica, iron oxides and clay contents have an effect on the pore size. Pore lining iron oxides and clay content have an effect on the pore throat radius. Both the pore size and the distribution of pore throat radius have a strong effect on the porosity–permeability relationship.

3.3. P-wave velocity of dry rock samples

The measured P-wave values of dry rock samples (Vp-dry) vary from 2289 to 3391 m/s with a mean value of 2766 m/s and a standard deviation 308 m/s.

The relationship between P-wave velocity of dry rock samples and porosity is displayed in Fig. 3. It shows a weak to fair inverse relationship with correlation coefficient $r = 0.46$,

$$\text{Vp-dry} = 4043 - 4380\Phi \text{ m/s} \quad (10)$$

The relationship of P-wave of dry rock samples and permeability, which is shown in Fig. 4, illustrates that the data points result in a cloud of points with no clear trend.

The direct proportional relationship between P-wave velocity of dry rock samples and dry bulk density, which is displayed in Fig. 5, shows a fair direct proportional relationship with correlation coefficient of $r = 0.56$.

$$\text{Vp-dry} = 1853 d_b - 734 \text{ m/s} \quad (11)$$

The relationships of P-wave velocity of dry rock samples with porosity, permeability and dry bulk density indicate that porosity and dry bulk density control P-wave velocity of dry rock samples to some extent, while permeability seems not related to P-wave velocity.

3.4. P-wave velocity of wet rock samples

The measured P-wave values of wet samples (Vp-wet) vary from 2528 to 3572 m/s, with mean values 2950 m/s and standard deviation 242 m/s.

The relationship between P-wave velocity of wet rock samples and porosity was plotted in Fig. 6. The relationship was improved to be better than that in the dry case, where the correlation coefficient became $r = 0.62$,

$$\text{Vp-wet} = 4306 - 4636\Phi \text{m/s} \tag{12}$$

The porosity can be estimated based on the generalized velocity–porosity relation (modified Raymer equation) if porosity should be estimated from P-wave velocities for both dry and saturated conditions.

$$v = (1-\Phi)^a v_s + \Phi^b v_f \tag{13}$$

with v being the velocity of the rock, versus the velocity of the solid material, v_f the velocity of the pore fluid, while a and b representing varying exponents in a common family tree of velocity–porosity relations, [23]. A special member of this family of equations with $a = 2$ and $b = 1$ was investigated by Raymer et al. [22]. The exponent of the solid fraction, which is 2 in the Raymer equation, has to be increased at 3 for saturated and at 3.4 for dry conditions. The exponent of the pore fraction (porosity) remains close to one [17].

The relationship of P-wave of wet rock samples and permeability, which is displayed in Fig. 7 illustrates that the data points result in a cloud of points with no clear relationship.

The relationship between P-wave of wet rock samples and wet bulk density, which is displayed in Fig. 8, shows a good relationship, which is better than that in the dry case, where correlation coefficient increases to $r = 0.77$.

$$\text{Vp-wet} = 2797 d_w - 3151 \text{ m/s} \tag{14}$$

The relationships of P-wave velocity of wet rock samples with porosity, permeability and wet bulk density show a similar behavior compared to the P-wave velocity of dry samples. The relationships of P-wave velocity of wet rock samples with porosity and wet bulk density have been improved after saturation, compared to the P-wave velocity of dry samples, where the correlation coefficients increase.

3.5. S-wave velocity of dry rock samples

The measured S-wave velocity values of dry rock samples (Vs-dry) vary from 1034 to 2401 m/s with a mean value of 1585 m/s and standard deviation 343 m/s.

The relationship between S-wave velocity of dry rock samples and porosity is displayed in Fig. 9. The resulting data points are flocked together in a cloud of points without any clear trend.

The relationship of S-wave of dry rock samples and permeability, which is displayed in Fig. 10, does not show any trend.

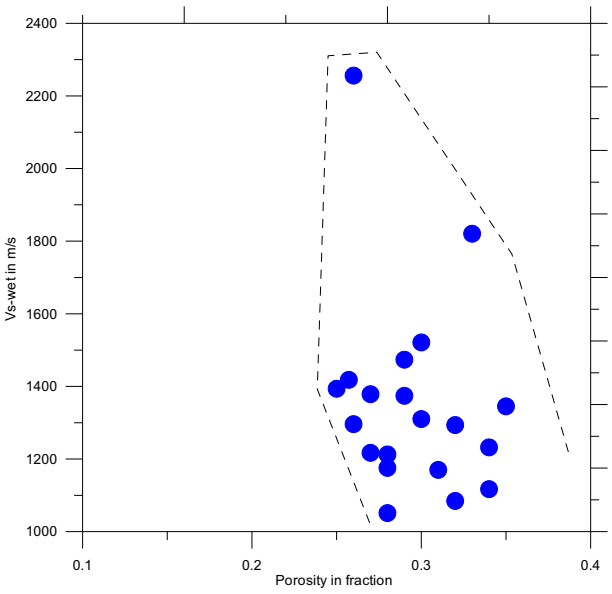

Figure 12 Relationship between porosity and S-wave velocity of wet rock samples.

The relationship between S-wave velocity of dry rock samples and dry bulk density, which is plotted in Fig. 11, shows a very weak direct proportional relationship. The plot indicates a slight increase in S-wave velocity of dry rock samples with increasing dry density.

3.6. S-wave velocity of wet rock samples

The S-wave velocity values of wet rock samples (Vs-wet) vary from 1051 to 2256 m/s with a mean value of 1357 m/s and a standard deviation 267 m/s.

The relationship between S-wave velocity of wet rock samples and porosity, which is displayed in Fig. 12, shows a very weak inverse relationship.

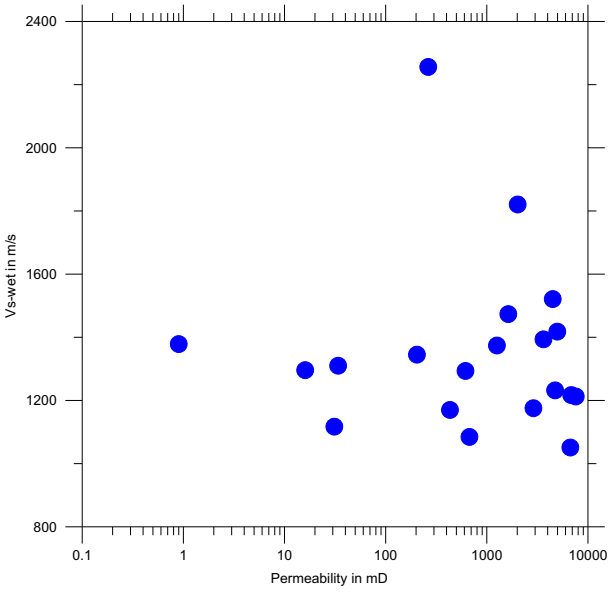

Figure 13 Relationship between permeability and S-wave velocity of wet rock samples.

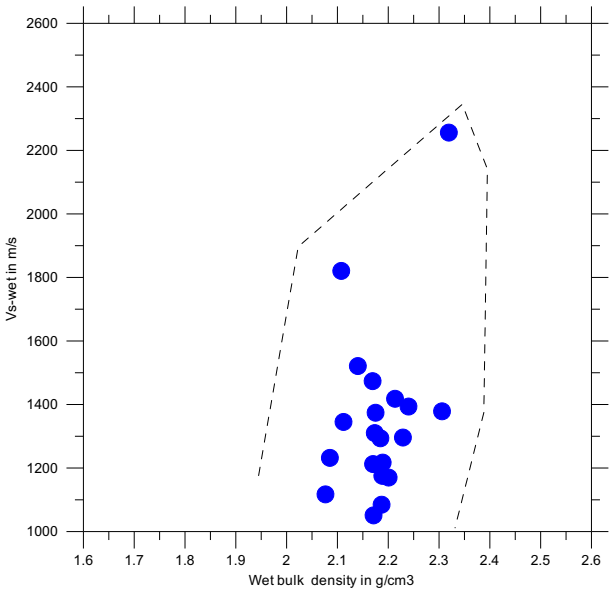

Figure 14 Relationship between S-wave velocity and wet bulk density of wet rock samples.

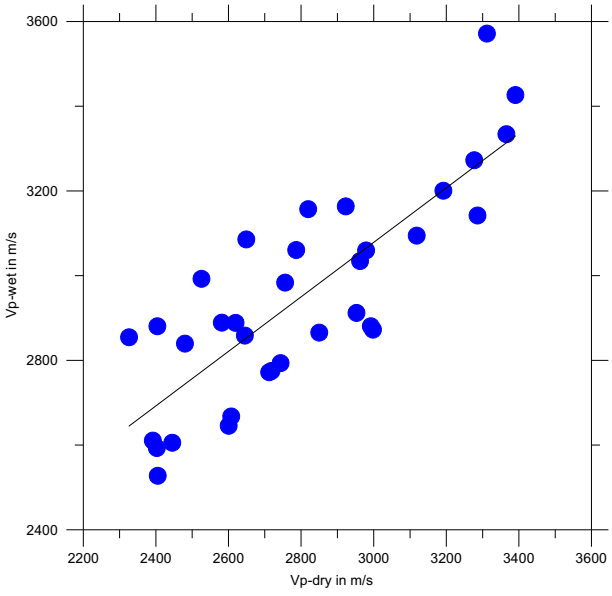

Figure 15 Relationship between P-wave velocity of dry rock samples and P-wave velocity of wet rock samples.

The comparison of S-wave of wet rock samples and permeability, which is shown in Fig. 13, does not show any clear trend.

The cross plot of S-wave velocity of wet rock samples and wet density in Fig. 14 exhibits a scatter of data points that is similar to the cross plot of S-wave velocity against the dry density in Fig. 11. The two plots indicate only a very weak positive trend.

3.7. P-wave velocity of dry rock samples and P-wave velocity of wet rock samples relationship

The comparison between P-wave velocity of dry rock samples and P-wave velocity of wet rock samples, which is displayed in Fig. 15, shows a very good direct proportional relationship with a correlation coefficient of $r = 0.82$, which means that the P-wave velocity of wet rock samples can be predicted from the P-wave velocity of dry rock samples with a high precision.

$$\text{Vp-wet} = 0.64\text{Vp-dry} + 1148 \text{ m/s} \quad (15)$$

3.8. S-wave velocity of dry rock samples and S-wave velocity of wet rock samples relationship

The comparison between S-wave velocity of dry rock samples and S-wave velocity of wet rock samples, which is plotted in Fig. 16, indicates a very good direct proportional relationship with a correlation coefficient of $r = 0.84$. The S-wave velocity of wet rock samples can be well predicted from the S-wave of dry rock samples with a reliable accuracy.

$$\text{Vs-wet} = 0.65\text{Vs-dry} + 321 \text{ m/s} \quad (16)$$

3.9. P-wave velocity of dry rock samples and S-wave velocity of dry rock samples relationship

Fig. 17 compares P-wave velocity and S-wave velocity of dry rock samples. The graph exhibits a good direct proportional relationship with a correlation coefficient of $r = 0.65$. This relationship indicates that S-wave velocity of dry rock samples can be calculated from P-wave velocity of dry rock samples.

$$\text{Vs-dry} = 0.73\text{Vp-dry} + 494 \text{ m/s} \quad (17)$$

3.10. P-wave velocity of wet rock samples and S-wave velocity of wet rock samples relationship

The comparison between P-wave velocity and S-wave velocity of wet rock samples as shown in Eq. (18) with a correlation coefficient of $r = 0.62$, indicates that S-wave velocity of wet

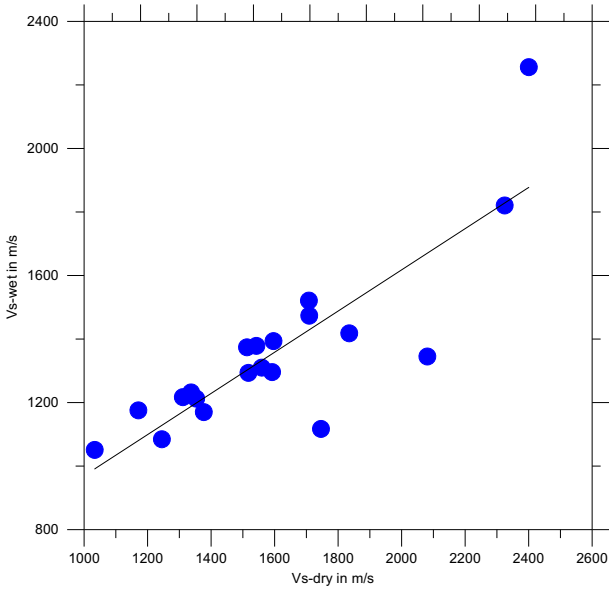

Figure 16 Relationship between S-wave velocity of dry rock samples and S-wave velocity of wet rock samples.

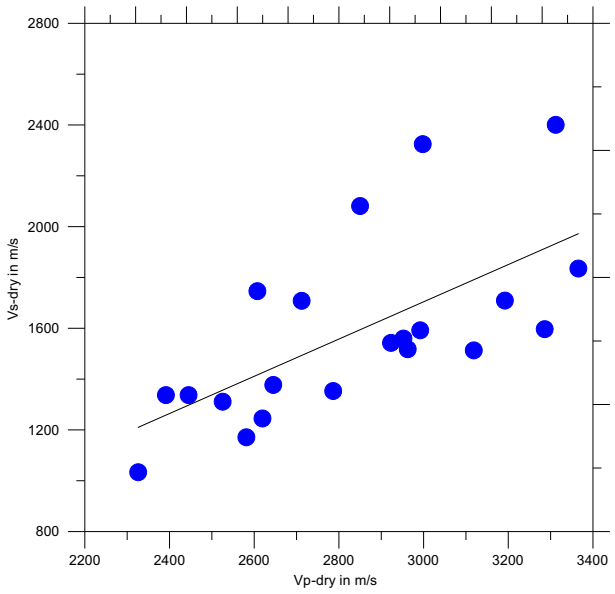

Figure 17 Relationship between P-wave velocity and S-wave velocity of dry rock samples.

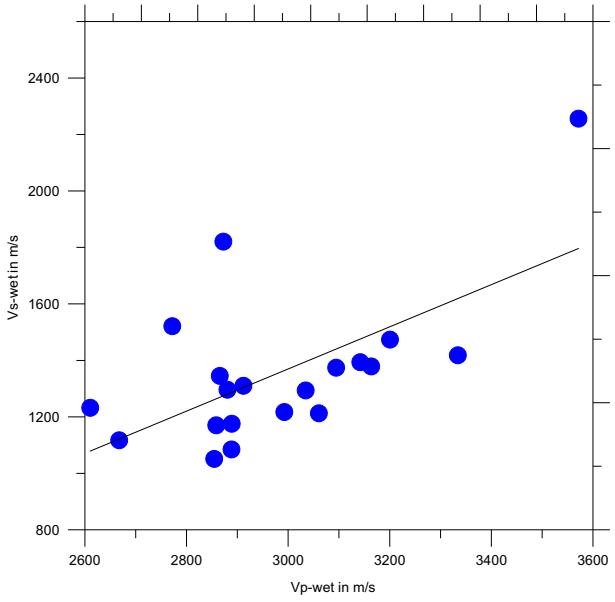

Figure 18 Relationship between P-wave velocities and S-wave velocity of wet rock samples.

rock samples can be simply estimated from P-wave velocity of wet rock samples (Fig. 18).

$$\text{Vs-wet} = 0.75\text{Vp-wet} - 871 \text{ m/s} \quad (18)$$

4. Conclusion

The studied sandstones are represented by quartz arenite composed of quartz grains cemented together by silica, iron oxides, and/or clay content. The cementation sometimes slightly reduces porosity. Dissolution and leaching out of quartz, clay contents and feldspar are the main porosity enhancing diagenetic factors giving rise to excellent porosity and permeable paths for pore fluid movement.

The relationship between porosity and permeability for the rock samples is affected by cementation with silica, iron oxides and/or clay content, (Plate 1A, B, D and E). The pore filling silica, iron oxides and/or clay content have an effect on the pore size. Pore lining iron oxides and clay contents have an effect on the pore throat radius. Both the pore size and the distribution of pore throat radius have a strong effect on the porosity–permeability relationship. The theoretical relation between porosity and dry bulk density can be used to predict porosity from bulk density if the grain density is known.

The investigated relationships of porosity versus seismic velocities, permeability versus seismic velocities and density versus seismic velocities for both dry and wet rock samples indicate poor to fair relationships. The resulting relationships indicate that porosity and density affect both P-wave and S-wave velocities. The relationships between permeability and seismic velocities could not be identified. Besides these petrophysical parameters, seismic velocities are mainly controlled by rock texture and mineral composition.

The statistical analysis indicate that the P-wave velocity is higher in the fully saturated state, where the average value of P-wave of wet rock samples is 2950 m/s and P-wave of dry rock samples is 2766 m/s. The S-wave velocity is higher in the dry state, where the average S-wave velocity of dry rock samples is 1585 m/s and the average S-wave velocity of wet rock samples is 1357 m/s. The increase in P-wave velocity and decrease in S-wave velocities with increasing saturation are in agreement with Gassmann's theory [11].

The relationships indicate that the P-wave velocity of wet rock samples is strongly correlated with the P-wave velocity of dry rock samples, and the derived equations can be used for the prediction of the P-wave velocity of wet rock from the P-wave velocity of dry rock. The S-wave velocity of wet rock samples is strongly correlated with the S-wave velocity of dry rock samples, too. The derived equations can be used for the prediction of the S-wave velocity of wet rock from the S-wave of dry rock.

The resulting linear relations between S-wave velocity and P-wave velocity of both dry and wet rock samples are characterized by high correlation coefficients for both dry and wet rock samples. The linear equations enable the estimation of S-wave velocity from P-wave velocity for both dry and wet rock.

Acknowledgments

M.K. thanks Egyptian Missions (Ministry for Higher Education, Research and Technology) for a post-doctoral scholarship that enabled the joint research between Egyptian Petroleum Research Institute, Cairo, Egypt, and the Institute of Geophysics at Clausthal University of Technology, Germany. The authors thank Dr. Wolfgang Debschütz and Dr. Carl-Dietrich Sattler for their support during the investigation and interpretation.

References

[1] J.W. Amyx, D.M. Bass Jr., R.L. Whiting, Petroleum Reservoir Engineering, Mc Graw Hill Publ. Co., New York, 1960, 601p.

[2] M.I. Attia, Geol. Surv., Egypt, 1955, 262p.
[3] M.A. Biot, J. Acoust. Soc. Am. 28 (1956) 179–191.
[4] A. Boulanouar, A. Rahmouni, M. Samaouali, Y. Géraud, M. Harnafi, J. Sebbani, Geomaterials 3 (2013) 138–144, Published Online October 2013.
[5] H. Brandt, ASME J. Appl. Mech. 22 (1955) 479–486.
[6] S. El Akkad, B. Issawi, Geol. Surv. Egypt, Pap. 18 (1963), 301p..
[7] A. El Monem, I. El Aassy, O. Hegab, I. El Fayoumy, N. El Agamy, Sedimentol. Egypt 5 (1997) 117–132.
[8] A.A. El Sayed, I. Berezi, B. Kiss, J. Appl. Geophys. 3 (2004) 95–105.
[9] A.A. El Sayed, M. El Batanony, A. Salah, in: MinChem '98, 27–30 September, Siofok, Hungary, 1998, pp. 9–14.
[10] R.L. Folk, Petrology of Sedimentary Rocks, Hemphill Publishing Co., Austin, Texas, 1974, 182p.
[11] F. Gassmann, Vierteljahrsschr der Naturforschenden Gesselschaft 96 (1951) 1–23.
[12] A.R. Gregory, Geophysics 41 (1976) 895–921.
[13] D.H. Han, A. Nur, D. Morgan, Geophysics 51 (1986) 2093–2107.
[14] W.G. Hicks, J.E. Berry, Geophysics 21 (1956) 739–754.
[15] D.S. Hughes, J.L. Kelly, Geophysics 17 (1952) 739–752.
[16] S. Kahraman, Ultrasonics 46 (2007) 341–348.
[17] M.A. Kassab, A. Weller, J. Pet. Sci. Eng. 78 (2011) 310–315.
[18] M.A. Kassab, A. Weller, J. Earth Sci. Eng. 5 (2013) 314–321.
[19] M.J. Minear, in: Presented at the 57th Ann. Mtg., Am. Inst. Min. Metall. Eng., New Orleans, 1982.
[20] B.S. Nabawy, P. Rochette, Y. Ǵeraud, Geophys. J. Int. 183 (2010) 681–694.
[21] F.J. Pettijohn, P.E. Potter, R. Siever, Sand and Sandstone, second ed., Springer-Verlag, New York, 1987, 553p..
[22] D.S. Raymer, E.R. Hunt, J.S. Gardner, Proc. SPWLA 21st Ann. Meeting (1980) 1–13.
[23] J.H. Schön, Physical Properties of Rocks: Fundamentals and Principles of Petrophysics, Elsevier, Oxford, 1996, 582p..
[24] Schlumberger, Log Interpretation Principles/Applications, Schlumberger Educational Services, Houston, Texas, 1989, 223p.
[25] G.K. Thabit, Sedimentology of the Nubia Group in the Area Southwest of Aswan, Abu Simbil Area (M.Sc. thesis), Assuit University, Egypt, 1994.
[26] A. Weller, M.A. Kassab, W. Debschütz, C.-D. Sattler, Arabian J. Geosci. (2013), http://dx.doi.org/10.1007/s12517-013-1188-7.